PHYSICAL REVIEW E **91**, 030801(R) (2015)

Reconstructing weighted networks from dynamics

Emily S. C. Ching,[1,*] Pik-Yin Lai,[2,3,†] and C. Y. Leung[1,‡]

[1]*Department of Physics, The Chinese University of Hong Kong, Shatin, Hong Kong*

[2]*Department of Physics and Center for Complex Systems, National Central University, Chungli, Taiwan 320, Republic of China*

[3]*Physics Division, National Center for Theoretical Sciences, Kuang Fu Road 101, Hsinchu, Taiwan 300, Republic of China*

(Received 12 June 2014; revised manuscript received 6 February 2015; published 24 March 2015)

We present a method that reconstructs both the links and their relative coupling strength of bidirectional weighted networks. Our method requires only measurements of node dynamics as input. Using several examples, we demonstrate that our method can give accurate results for weighted random and weighted scale-free networks with both linear and nonlinear dynamics.

DOI: 10.1103/PhysRevE.91.030801 PACS number(s): 89.75.Hc, 05.45.Tp, 05.45.Xt

Many multicomponent systems of interest in physics, biology, or social science are complex networks with the components being the nodes or vertices and the interactions between components being the links or edges [1–3]. The links and their weights or relative coupling strength are important basic features of a network that provides insights and fundamental understanding of the overall behavior and functionality of the network. A vast amount of data has been measured for various networks of interest such as gene regulatory [4,5] and brain networks [6] but it remains a challenge to reconstruct a network, i.e., finding the links and their relative coupling strength, from these measurements. All existing network reconstruction methods have their limitations [7,8]. Many existing methods are statistical in nature, inferring the links from statistical correlations [9] and dependence [10] of the measurements of the nodes or employing Bayesian graphical models [4,11,12] to find the network that best matches the measured statistics. Statistical correlation and dependence, however, does not necessarily follow from direct connections, and the matching problem is underdetermined as the number of possible answers far exceeds the number of available measurements. It has been suggested [13] that the topology of a network controls its dynamics and thus information about the network connectivity can be uncovered from their dynamics. We have recently developed [14] a method that reconstructs the links of bidirectional networks with uniform strength of interaction. Our method uses only measurements of nodal dynamics as input and is shown to give accurate results for various networks with both linear and nonlinear dynamics. Earlier methods [15] either assume linearity [16,17] or require additional information [18–22]. In realistic networks, the strength of interaction often differs for different pairs of nodes, and these networks are weighted [23]. Reconstruction of weighted networks is even more challenging.

In this Rapid Communication, we present a method that reconstructs *both* the links and their weights of bidirectional weighted networks. Our method requires only measurements of nodal dynamics as input. Using various examples, we demonstrate that our method gives accurate results for weighted random and weighted scale-free networks with both linear and nonlinear dynamics.

We consider bidirectional weighted networks of N nodes, each with a variable $x_i(t)$, $i = 1,2,\ldots,N$, and

$$\dot{x}_i = f(x_i) + \sum_{j\neq i} g_{ij} A_{ij} h(x_i,x_j) + \eta_i. \tag{1}$$

Here the overdot denotes derivative with respect to time t, and f describes the intrinsic dynamics, which is taken to be identical for all nodes. The adjacency matrix element A_{ij} is 1 when node j is linked to node i by the coupling function $h(x_i,x_j)$ with strength g_{ij}; otherwise $A_{ij} = g_{ij} = 0$. The coupling is bidirectional such that $A_{ij} = A_{ji}$ and $g_{ij} = g_{ji}$. We assume that the graphs of the networks have one connected part and no self-loops such that $A_{ii} \equiv 0$. We model external disturbances by a Gaussian white noise with zero mean and variance σ^2: $\overline{\eta_i(t)\eta_j(t')} = \sigma^2\delta_{ij}\delta(t-t')$, where the overbar is an average over different realizations of the noise. Our goal is to reconstruct A_{ij} and g_{ij} using only $x_i(t)$.

We define the matrix M by

$$M_{ij} = \frac{s_i}{\langle g\rangle}\delta_{ij} - \frac{g_{ij}A_{ij}}{\langle g\rangle}, \qquad s_i \equiv \sum_{j=1}^{N} g_{ij}A_{ij}, \tag{2}$$

where $\langle g\rangle \equiv \sum_{i,j} g_{ij}A_{ij}/\sum_{i,j} A_{ij}$ is the average coupling strength and s_i is the strength of node i. M is the normalized Laplacian matrix of a weighted network and contains all the information of A_{ij} and g_{ij}. Using $x_i(t)$, we calculate the dynamical covariance matrix C with

$$C_{ij} = \langle [x_i(t) - X(t)][x_j(t) - X(t)]\rangle_T, \tag{3}$$

where $X(t) \equiv (1/N)\sum_{i=1}^{N} x_i(t)$ and $\langle\cdots\rangle_T$ is an average over a time interval T of the measurements. We first show an approximate relation between the pseudoinverse of C, denoted as C^+, and M for networks with positive semidefinite M and $h(x,y)$ satisfying

$$h(x,y) = h(z), \qquad h(-z) = -h(z), \qquad h'(0) > 0\,, \tag{4}$$

where $z = y - x$. With such a coupling function, the dynamics of the nodes tend to synchronize such that x_i's approach a stable fixed point X_0 in the noise-free limit given by $f(X_0) = 0$ and $f'(X_0) < 0$. In the presence of weak noise, $\delta x_i = x_i - X_0$

*ching@phy.cuhk.edu.hk

†pylai@phy.ncu.edu.tw

‡Present address: School of Biology and School of Physics, Georgia Institute of Technology, Atlanta, GA.

is small and we have

$$\dot{\delta x_i} \approx -\langle g\rangle h'(0)\sum_{j=1}^{N}\left(M_{ij}-\frac{f'(X_0)}{\langle g\rangle h'(0)}\delta_{ij}\right)\delta x_j+\eta_i. \quad (5)$$

Following the ideas of the proof given in [14], we derive an exact result between C^+ and M in the limit $T\to\infty$ for the linearized system (5), which is an approximation for the system (1) with (4):

$$\frac{\sigma^2}{2\langle g\rangle h'(0)}\lim_{T\to\infty}\overline{C}_{ij}^{+}\approx M_{ij}-\frac{f'(X_0)}{\langle g\rangle h'(0)}\left(\delta_{ij}-\frac{1}{N}\right), \quad (6)$$

with the factor $\delta_{ij}-1/N$ coming from $\sum_k M_{ik}^{+}M_{kj}$. For consensus dynamics [24], defined by $f=0$ and $h(z)=z$, relation (6) becomes $\sigma^2/(2\langle g\rangle)\lim_{T\to\infty}\overline{C}_{ij}^{+}=M_{ij}$ and is exact [25].

Guided by relation (6), we devise a method to reconstruct A_{ij} and g_{ij}. Approximating $\lim_{T\to\infty}\overline{C}_{ij}^{+}$ by C_{ij}^{+} with a finite $T=T_{\rm av}$ and using Eq. (2), we get

$$r_{ij}\equiv\frac{C_{ij}^{+}}{C_{ii}^{+}}\approx\begin{cases}\dfrac{-g_{ij}}{s_i-f'(X_0)/h'(0)}, & A_{ij}=1\\ 0, & A_{ij}=0\end{cases} \quad (7)$$

for $i\neq j$, where we have neglected the $1/N$ term for large networks. For each node i, r_{ij} for nodes j connected to i would have gaps among themselves because of different g_{ij} and also have a gap from those unconnected to node i. By identifying the latter gap [26], we obtain the reconstructed $A_{ij}^{(e)}$. Moreover, Eq. (6) implies

$$-(\sigma^2/2)C_{ij}^{+}\approx h'(0)g_{ij},\qquad i\neq j, \quad (8)$$

which further implies

$$G_{ij}\equiv\frac{g_{ij}}{\langle g\rangle}\approx\frac{C_{ij}^{+}\sum_l k_l^{(e)}}{\sum_{n,l\leftrightarrow n}C_{nl}^{+}}\equiv G_{ij}^{(e)}, \quad (9)$$

$$S_i\equiv\frac{s_i}{\langle s\rangle}=\frac{\sum_j G_{ij}A_{ij}}{\langle k\rangle}\approx\frac{N\sum_{j\leftrightarrow i}C_{ij}^{+}}{\sum_{n,l\leftrightarrow n}C_{nl}^{+}}\equiv S_i^{(e)}, \quad (10)$$

where $\langle s\rangle\equiv\sum_i s_i/N$, $k_i=\sum_{j=1}^{N}A_{ij}$ is the degree of node i, $\langle k\rangle\equiv\sum_i k_i/N$, $k_i^{(e)}=\sum_{j=1}^{N}A_{ij}^{(e)}$ is the reconstructed degree of node i, and $\sum_{l\leftrightarrow n}$ represents a sum over nodes l that are reconstructed to be connected to node n. We use Eqs. (9) and (10) to obtain the reconstructed relative coupling strength $G_{ij}^{(e)}$ and relative strength of nodes $S_i^{(e)}$.

We apply our method to two weighted random (WR) networks of $N=100$ with a connection probability of 0.2 and two different weighted scale-free (WSF) networks of $N=1000$. The two WR networks have g_{ij} taken from two Gaussian distributions of different mean μ and standard deviation γ: $\mu=5$ and $\gamma=2$ (WR1) and $\mu=10$ and $\gamma=2$ (WR2). The WSF networks are two different extensions [27,28] of the (unweighted) Barabasi-Albert SF network [29], and are generated by starting with $n=5$ nodes and adding a new node to $m=5$ different existing nodes at each step. The probability of connecting to an existing node i is either proportional to k_i [27] (WSF1) or s_i [28] (WSF2). For WSF1, the coupling strength of a new link is $g_{ij}=g_0k_i/\sum_{i'}k_{i'}$, where $g_0=10$ and $\sum_{i'}$ is over the existing nodes i' that the new node j is connected. For WSF2, the new link changes the coupling strength g_{ij} of all the other links of the existing node i to $g_{ij}(1+\delta/s_i)$ with $\delta=2$. The degree distribution $P(k)$ is a power law with an exponent -3 (WSF1) or $-(4\delta+3)/(2\delta+1)$ (WSF2). The relative coupling strength distribution $P(G)$ has a peak and is skewed for WSF1 but is a power law for WSF2.

To test the general applicability of the method, we study not only the linear consensus dynamics and nonlinear intrinsic logistic dynamics $f(x)=rx(1-x)$ with $r=10$ and $h(z)=z$ (logistic) for which (6) is expected to hold, but also nonlinear coupling function that cannot be linearized: $f=0$ and $h(z)=z^3$ (cubic), and higher-dimensional dynamics with different coupling. We study the FitzHugh-Nagumo (FHN) dynamics [30]:

$$\dot{x}_i=\left(x_i-x_i^3/3-y_i\right)/\epsilon+\sum_{j\neq i}g_{ij}A_{ij}h(x_i,x_j)+\eta_i, \quad (11)$$

$$\dot{y}_i=x_i+\alpha \quad (12)$$

with both $h(x,y)=h(z)=z$ and $\alpha=1.05$ (FHN1) or $\alpha=0.95$ (FHN2) and synapticlike coupling $h(x,y)=\{1+\tanh[\beta(y-x_{\rm th})]\}/2$ with $\beta=2$ and $x_{\rm th}=1$ and $\alpha=1.05$ (FHN3), together with $\epsilon=0.01$, as well as the Rössler dynamics [31]:

$$\dot{x}_i=-y_i-z_i+\sum_{j\neq i}g_{ij}A_{ij}\tanh[(x_j-x_i)]+\eta_i, \quad (13)$$

$$\dot{y}_i=x_i+ay_i+\sum_{j\neq i}g_{ij}A_{ij}\tanh[(y_j-y_i)], \quad (14)$$

$$\dot{z}_i=b+z_i(x_i-c)+\sum_{j\neq i}g_{ij}A_{ij}\tanh[(z_j-z_i)]. \quad (15)$$

TABLE I. Accuracy of $A_{ij}^{(e)}$ measured by $P_{\rm SEN}$ and $P_{\rm SPEC}$ for the networks and dynamics studied.

Network	Dynamics	$T_{\rm av}$	$P_{\rm SEN}$ (%)	$P_{\rm SPEC}$ (%)
WR1	Consensus	1000	94.3	100.00
WR1	Rössler	1000	94.2	100.00
WR1	FHN3	1000	26.9	99.57
WR1	FHN3	5000	52.6	99.70
WR2	Logistic	1000	99.9	100.00
WR2	Cubic	1000	96.8	99.70
WR2	FHN1	1000	99.5	100.00
WR2	FHN2	1000	98.1	99.97
WSF1	Consensus	1000	88.3	99.98
WSF1	Rössler	1000	86.0	99.99
WSF1	FHN1	1000	56.8	99.83
WSF1	FHN1	5000	85.5	99.87
WSF1	FHN2	1000	61.4	99.80
WSF1	FHN2	5000	85.7	99.86
WSF2	Consensus	1000	91.7	99.98
WSF2	Rössler	1000	85.2	99.98
WSF2	FHN1	1000	34.9	99.69
WSF2	FHN1	5000	86.7	99.98
WSF2	FHN2	1000	37.5	99.73
WSF2	FHN2	5000	83.3	99.98

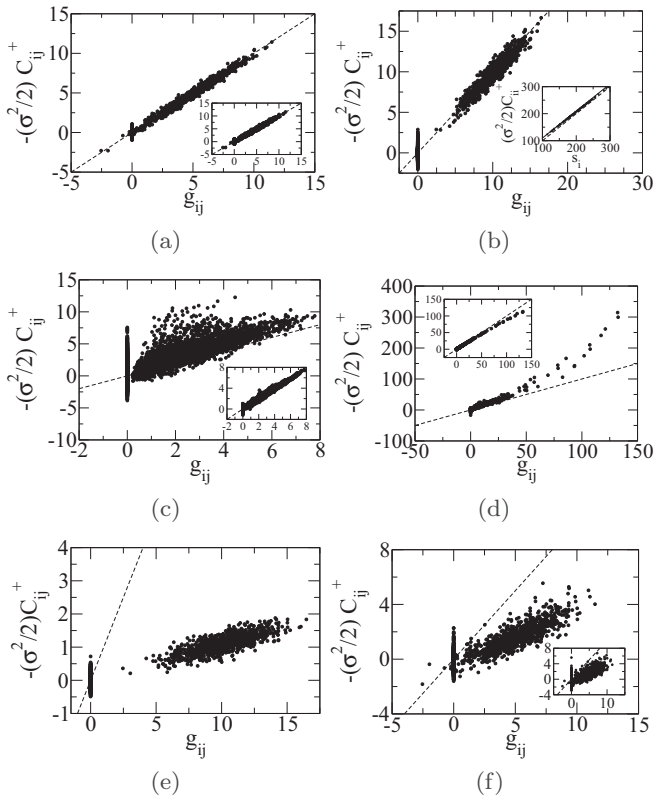

FIG. 1. $-(\sigma^2/2)C_{ij}^+$ versus g_{ij} for (a) WR1 with Rössler and consensus (inset) dynamics, (b) WR2 with logistic dynamics (inset shows $\sigma^2/2C_{ii}^+$ versus s_i with solid line for the theoretical result [Eq. (6)]), (c) WSF1 with FHN1 and Rössler (inset) dynamics, (d) WSF2 with FHN2 and consensus (inset) dynamics, (e) WR2 with cubic coupling, and (f) WR1 with FHN3 dynamics for $T_{\rm av} = 5000$ and $T_{\rm av} = 1000$ (inset). In all the other cases, $T_{\rm av} = 1000$. Dashed line is $y = x$.

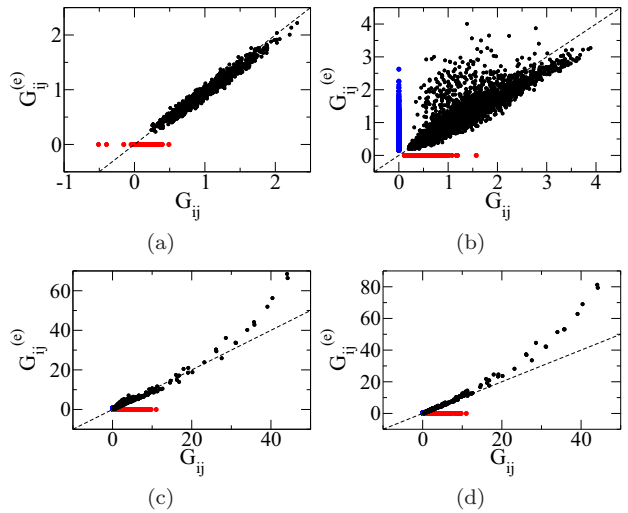

FIG. 2. (Color online) Comparison of the reconstructed $G_{ij}^{(e)}$ with the actual G_{ij} for (a) WR1 with Rössler dynamics, (b) WSF1 with FHN1 dynamics, (c) WSF2 with FHN2 dynamics, and (d) WSF2 with Rössler dynamics. $T_{\rm av} = 1000$ for (a) and (d) and $T_{\rm av} = 5000$ for (b) and (c). Undetected links have $G_{ij}^{(e)} = 0$ but $G_{ij} \neq 0$ while links with $G_{ij} = 0$ but $G_{ij}^{(e)} \neq 0$ are incorrectly reconstructed. The average absolute error of nonzero $G_{ij}^{(e)}$ is less than 7% for (a), less than and about 20% for (b) and (c), and about 10% for (d).

The parameters are $a = b = 0.2$ and $c = 9$, chosen such that the Rössler dynamics is chaotic without the coupling and noise. We take $\sigma = 1$ in all the cases studied and numerically integrate the equations of motion using either the Euler-Maruyama method or the weak second-order Runge-Kutta method [32]. For the FHN and Rössler dynamics, we reconstruct the networks using $x_i(t)$ only. The sampling interval of $x_i(t)$ is 5×10^{-4} for all the cases.

We measure the accuracy of $A_{ij}^{(e)}$ by the percentages of correctly reconstructed links and nonexistent links, denoted by $P_{\rm SEN}$ and $P_{\rm SPEC}$, respectively (Table I). Using ten different realizations of the WR1 network, we check that the standard deviation of $P_{\rm SEN}$ and $P_{\rm SPEC}$ is less than 2%. As our identification of the gaps [26] tends to be more stringent, $P_{\rm SEN}$ is generally smaller than $P_{\rm SPEC}$. There are two general results: (i) the reconstruction is more accurate for the WR than the WSF networks with the same dynamics, and (ii) the accuracy is increased when $T_{\rm av}$ is increased. Our method gives rather accurate results: except for WR1 with FHN3 dynamics, both $P_{\rm SEN}$ and $P_{\rm SPEC} > 80\%$ when $T_{\rm av}$ is at most 5000. In the WSF networks, small-degree nodes connected to large-degree nodes have a large disparity in g_{ij}. The presence of links with dominantly large coupling strength makes it easier to miss the other links with moderate coupling strength in our method [26] and thus reduces $P_{\rm SEN}$. This explains the general result (i). Moreover, the number of errors for individual nodes increases as $(\min_j\ g_{ij})/s_i$ decreases as expected from Eq. (7).

Next we study the dependence of $-(\sigma^2/2)C_{ij}^+$ on g_{ij} for $i \neq j$ (see Fig. 1). We find that the data points scatter around the line $y = x$, confirming Eq. (8), not only for consensus and logistic dynamics with $h'(0) = 1$ as expected but also for higher-dimensional Rössler dynamics for WR1 and WSF1 and FHN1 dynamics for WR2. Our theoretical result, Eq. (6), for $i = j$ is also confirmed for WR2 with logistic dynamics [see inset of Fig. 1(b)]. In the other cases, although Eq. (8) does not hold, $-(\sigma^2/2)C_{ij}^+$ is approximately proportional to g_{ij} albeit with a much larger data scatter, particularly for $g_{ij} = 0$, except for the small number of very large g_{ij} for WSF2 with Rössler, FHN1, and FHN2 dynamics [see Fig. 1(d)]. These interesting observations suggest the approximate result

$$-(\sigma^2/2)C_{ij}^+ \approx Bg_{ij}. \qquad i \neq j \tag{16}$$

for general dynamics with some $B > 0$. When the data scatter for $g_{ij} = 0$ is large, C_{ij}^+ for $g_{ij} = 0$ would overlap significantly with those for $g_{ij} > 0$, resulting in a large number of incorrectly reconstructed links and thus a low $P_{\rm SEN}$. This explains the low $P_{\rm SEN}$ for WR1 with FHN3 dynamics for which $B \approx 0.3$. The data scatter is decreased when $T_{\rm av}$ is increased [see Fig. 1(f)] leading to the general result (ii). Note that Eqs. (9) and (10) remain valid when Eq. (16) holds. We compare $G_{ij}^{(e)}$ with the actual G_{ij}. Except for the small number of very large G_{ij} for WSF2 with Rössler, FHN1, and FHN2 dynamics, $G_{ij}^{(e)} \approx DG_{ij}$ (see Fig. 2) but $G_{ij}^{(e)}$ can deviate from G_{ij} due to inaccurate $k_i^{(e)}$ when $P_{\rm SEN}$ is low. Moreover, the undetected links are of relatively small g_{ij}, thus

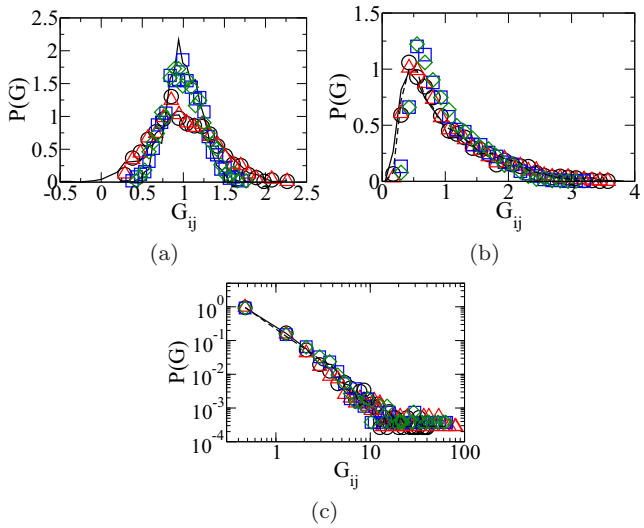

FIG. 3. (Color online) Comparison of $P(G)$ of the reconstructed $G_{ij}^{(e)}$ for consensus (circles), Rössler (triangles), FHN1 (squares), and FHN2 (diamonds) dynamics with $T_{\rm av} = 1000$ against the actual distribution (solid line) for (a) WR1 and WR2, (b) WSF1, and (c) WSF2 networks. Dashed line in (b) and (c) is the result for FHN2 dynamics with $T_{\rm av} = 5000$.

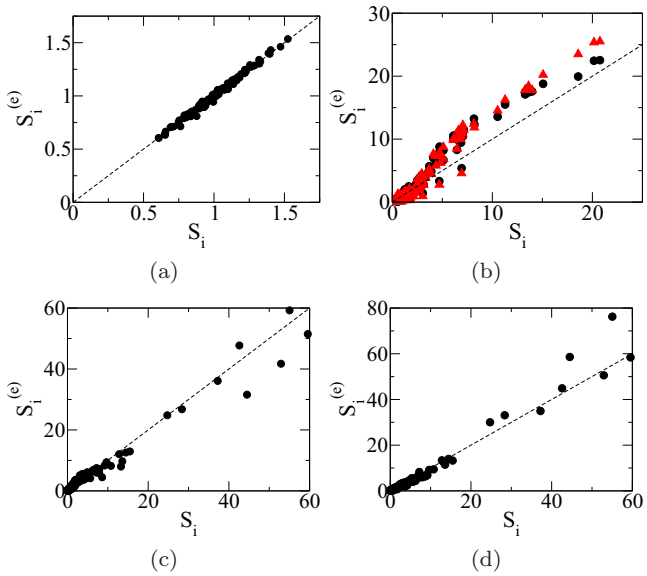

FIG. 4. (Color online) Comparison of the reconstructed $S_i^{(e)}$ (circles) and the actual S_i for (a) WR1 with Rössler dynamics, (b) WSF1 with FHN1 dynamics, (c) WSF2 with FHN2 dynamics, and (d) WSF2 with Rössler dynamics. In (b), we show also $(S_i^{(e)})_{\rm est}$ (triangles).

the reconstructed average coupling strength is overestimated resulting in an underestimation of G_{ij} and thus $D < 1$.

Then we compare the distribution $P(G)$ of the reconstructed $G_{ij}^{(e)}$ against the actual distribution. As shown in Fig. 3, our method captures the shape of $P(G)$ rather well and, in particular, reproduces both the peaked and skewed $P(G)$ of WSF1 and the power law in $P(G)$ of WSF2 even though it misses links of small G_{ij} and for WSF2 with Rössler, FHN1, and FHN2 dynamics, Eq. (16) does not hold for a small number of very large g_{ij}. The reconstructed $S_i^{(e)}$ is in very good agreement with the actual S_i except for WSF1 with FHN1 and FHN2 dynamics and for large S_i for WSF2 with Rössler, FHN1, and FHN2 dynamics (see Fig. 4). The fluctuation for large S_i for WSF2 is a result of the deviation of Eq. (16) for large g_{ij}. Using Eqs. (9) and (10), we obtain $S_i^{(e)}/S_i = [G_i^{(e)}/G_i][(k_i^{(e)}/k_i)(\langle k\rangle/\langle k\rangle^{(e)})]$, where $\langle k\rangle^{(e)} \equiv \sum_i k_i^{(e)}/N$, $G_i \equiv \sum_j G_{ij}A_{ij}/k_i$ is the average relative coupling strength of the links of node i, and $G_i^{(e)} \equiv \sum_j G_{ij}^{(e)}A_{ij}^{(e)}/k_i^{(e)}$ is the reconstructed value. By fitting $G_i^{(e)} = EG_i$ we get an estimate $(S_i^{(e)})_{\rm est} \equiv E[(k_i^{(e)}/k_i)(\langle k\rangle/\langle k\rangle^{(e)})]$, which captures well the observed $S_i^{(e)}$ [see Fig. 4(b)], showing that the deviation of $S_i^{(e)}$ from S_i for WSF1 with FHN1 and FHN2 dynamics is due to the inaccuracy of $k_i^{(e)}$.

We have presented a method that reconstructs bidirectional weighted networks using only nodal dynamics. Equation (16) is the basis of why our method works. For networks whose dynamics is described by Eq. (1) with coupling function satisfying Eq. (4), we have derived Eq. (6) that leads to Eq. (8), a special case of Eq. (16) with $B = h'(0)$. Although we have no proof of how general Eq. (16) is, our numerical studies show that it holds also for some systems with higher-dimensional nonlinear FHN or Rössler dynamics and with nonlinear cubic or synapticlike coupling. Whenever Eq. (16) holds and the data scatter is small enough such that C_{ij}^{+} for $g_{ij} = 0$ would not overlap significantly with C_{ij}^{+} for $g_{ij} \neq 0$, our method can reconstruct accurately both the links and their relative coupling strength. Using several examples, we have demonstrated that our method gives accurate $P_{\rm SEN}$ and $P_{\rm SPEC}$ (>80%) and captures the shape of $P(G)$ for WR and WSF networks with both linear and nonlinear dynamics. We emphasize that the connectivity information of a network is contained in C^{+} and not C, and C^{+} is closely related to the inverse of the usual covariance matrix Σ^{-1}, where $\Sigma_{ij} = \langle[x_i(t) - \langle x_i(t)\rangle_T][x_j(t) - \langle x_j(t)\rangle_T]\rangle_T$. Our work thus further explains why weakly correlated nodes can interact strongly [33]. Finally we note that when the interactions and their strengths are known, a feedback method that controls networks to desired dynamical states can be designed and implemented [34,35].

The work of E.S.C.C. and C.Y.L. has been supported by the Hong Kong Research Grants Council under Grant No. CUHK 14300914 while that of P.Y.L. has been supported by Ministry of Science and Technology of Taiwan under Grant No. NSC 101-2112-M-008-004-MY3.

[1] S. H. Strogatz, Exploring complex networks, Nature (London) **410**, 268 (2001).

[2] R. Albert and A.-L. Barabási, Statistical mechanics of complex networks, Rev. Mod. Phys. **74**, 48 (2002).

[3] M. E. J. Newman, The structure and function of complex networks, SIAM Rev. **45**, 167 (2003).

[4] F. Emmert-Streib, G. V. Glazko, G. Altay, and R. de Matos Simoes, Statistical inference and reverse engineering of gene regulatory networks from observational expression data, Front. Genet. **3**, 1 (2012).

[5] G. Karlebach and R. Shamir, Modelling and analysis of gene regulatory networks, Nat. Rev. Mol. Cell Biol. **9**, 771 (2008).

[6] E. Bullmore and O. Sporns, Complex brain networks: Graph theoretical analysis of structural and functional systems, Nat. Rev. Neurosci. **10**, 186 (2009).

[7] R. De Smet and K. Marchal, Advantages and limitations of current network inference methods, Nat. Rev. Microbiol. **8**, 717 (2010).

[8] D. Marbach *et al.*, Wisdom of crowds for robust gene network inference, Nat. Methods **9**, 796 (2012).

[9] J. M. Stuart, E. Segal, D. Killer, and S. K. Jim, A gene-coexpression network for global discovery of conserved genetic modules, Science **302**, 249 (2003).

[10] L. M. A. Bettencourt, V. Gintautas, and M. I. Ham, Identification of Functional Information Subgraphs in Complex Networks, Phys. Rev. Lett. **100**, 238701 (2008).

[11] N. Friedman, M. Linial, I. Nachman, and D. Peer, Using Bayseian networks to analyze expression data, J. Comput. Biol. **7**, 601 (2000).

[12] S. M. Smith, K. L. Miller, G. Salimi-Khorshidi, Ma. Webster, C. F. Beckmann, T. E. Nichols, J. D. Ramsey, and M. W. Woolrich, Network modeling methods for FMRI, Neuroimage **54**, 875 (2011).

[13] M. Timme, Does dynamics reflect topology in directed networks?, Europhys. Lett. **76**, 367 (2006).

[14] E. S. C. Ching, P. Y. Lai, and C. Y. Leung, Extracting connectivity from dynamics of networks with uniform bidirectional coupling, Phys. Rev. E **88**, 042817 (2013); **89**, 029901(E) (2014).

[15] M. Timme and J. Casadiego, Revealing networks from dynamics: An introduction, J. Phys. A **47**, 343001 (2014).

[16] M. K. S. Yeung, J. Tegner, and J. J. Collins, Reverse engineering gene networks using singular value decomposition and robust regression, Proc. Natl. Acad. Sci. USA **99**, 6163 (2002).

[17] D. Napoletani and T. D. Sauer, Reconstructing the topology of sparsely connected dynamical networks, Phys. Rev. E **77**, 026103 (2008).

[18] D. Yu, M. Righero, and L. Kocarev, Estimating Topology of Networks, Phys. Rev. Lett. **97**, 188701 (2006).

[19] S. G. Shandilya and M. Timme, Inferring network topolgy from complex dynamics, New J. Phys. **13**, 013004 (2011).

[20] M. Timme, Revealing Network Connectivity from Response Dynamics, Phys. Rev. Lett. **98**, 224101 (2007).

[21] J. Ren, W.-X. Wang, B. Li, and Y.-C. Lai, Noise Bridges Dynamical Correlation and Topology in Coupled Oscillator Networks, Phys. Rev. Lett. **104**, 058701 (2010).

[22] Z. Levnajić and A. Pikovsky, Network Reconstruction from Random Phase Resetting, Phys. Rev. Lett. **107**, 034101 (2011).

[23] M. E. J. Newman, Analysis of weighted networks, Phys. Rev. E **70**, 056131 (2004).

[24] R. Olfati-Saber, J. A. Fax, and R. M. Murray, Consensus and cooperation in networked multi-agent systems, Proc. IEEE **95**, 215 (2007).

[25] A related result between the Fourier transform of the cross-correlation function of the nodal dynamics and the Laplacian matrix for consensus dynamics has been derived in S. Shahrampour and V. M. Preciado, Reconstruction of Directed Networks from Consensus Dynamics, American Control Conference, 1685 (2013) but there is no discussion on how to use it for network reconstruction.

[26] For each node i, we arrange r_{ij} in ascending order, denoted as $r_i(m)$ with $r_i(1)$ being the smallest and find $m_0(i)$, which is the largest value of m such that $d_i(m) = r_i(m+1) - r_i(m)$ exceeds some threshold (the mean value plus two standard deviations). Nodes j with r_{ij} belonging to $r_i(m)$ for $m \leqslant m_0(i)$ $[m > m_0(i)]$ are reconstructed to be connected (unconnected) to node i.

[27] S. H. Yook, H. Jeong, A.-L. Barabási, and Y. Tu, Weighted Evolving Networks, Phys. Rev. Lett. **86**, 5835 (2001).

[28] A. Barrat, M. Barthélemy, and A. Vespignani, Weighted Evolving Networks: Coupling Topology and Weight Dynamics, Phys. Rev. Lett. **92**, 228701 (2004).

[29] A.-L. Barabási and R. Albert, Emergence of scaling in random networks, Science **286**, 509 (1999).

[30] R. FitzHugh, Impulses and physiological states in theoretical models of nerve membrane, Biophys. J. **1**, 445 (1961).

[31] O. E. Rössler, An equation for continuous chaos, Phys. Lett. A **57**, 397 (1976).

[32] T. Sauer, Numerical solution of stochastic differential equations in finance, *Handbook of Computational Finance* (Springer, New York, 2012), pp. 529–550.

[33] E. Schneidman, M. J. Berry, R. Segev, and W. Bialek, Weak pairwise correlations imply strongly correlated network states in a neural population, Nature (London) **440**, 1007 (2006).

[34] *Handbook of Chaos Control*, 2nd ed., edited by E. Scholl and H. G. Schuster (Wiley-VCH, Weinheim, 2008).

[35] S. Sridhar, D. M. Le, Y. C. Mi, S. Sinha, P. Y. Lai, and C. K. Chan, Suppression of cardiac alternans by alternating-period-feedback stimulations, Phys. Rev. E **87**, 042712 (2013).